J|A|C|S COMMUNICATIONS

Published on Web 12/07/2010

Nanopore Detection of 8-Oxo-7,8-dihydro-2′-deoxyguanosine in Immobilized Single-Stranded DNA via Adduct Formation to the DNA Damage Site

Anna E. P. Schibel, Na An, Qian Jin, Aaron M. Fleming, Cynthia J. Burrows,* and Henry S. White*

Department of Chemistry, University of Utah, 315 South 1400 East, Salt Lake City, Utah 84112-0850, United States

Received October 21, 2010; E-mail: burrows@chem.utah.edu; white@chem.utah.edu

Abstract: The ability to detect DNA damage within the context of the surrounding sequence is an important goal in medical diagnosis and therapies, but there are no satisfactory methods available to detect a damaged base while providing sequence information. One of the most common base lesions is 8-oxo-7,8-dihydroguanine, which occurs during oxidation of guanine. In the work presented here, we demonstrate the detection of a single oxidative damage site using ion channel nanopore methods employing α-hemolysin. Hydantoin lesions produced from further oxidation of 8-oxo-7,8-dihydroguanine, as well as spirocyclic adducts produced from covalently attaching a primary amine to the spiroiminodihydantoin lesion, were detected by tethering the damaged DNA to streptavidin via a biotin linkage and capturing the DNA inside an α-hemolysin ion channel. Spirocyclic adducts, in both homo- and heteropolymer background single-stranded DNA sequences, produced current blockage levels differing by almost 10% from those of native base current blockage levels. These preliminary studies show the applicability of ion channel recordings not only for DNA sequencing, which has recently received much attention, but also for detecting DNA damage, which will be an important component to any sequencing efforts.

Oxidative stress in the cell underlies multiple age-related disorders, including cancer, heart, and neurological diseases.[1] Reactive oxygen species (ROS) arising from metabolism, inflammation, and environmental exposure to redox-active compounds lead to oxidation of many cellular components; those reactions occurring on DNA bases are of particular concern for their mutagenic potential.[2,3] Chief among these DNA base lesions is 8-oxo-7,8-dihydroguanine (OG, Figure 1), an oxidized base that exists at the level of ∼1 in 10^6 bases under normal cellular conditions[4] but at much higher levels under conditions of stress or in certain disease states.[5] Present methods for detection of OG most commonly involve (1) the comet assay,[6] which can be performed on a single cell, although the lesion specificity of the assay is not high, and (2) HPLC-MS/MS methods, which provide a more accurate count of specific lesions such as OG but require complete enzymatic digestion to nucleosides before analysis.[7] Neither of these methods yields sequence information,[8] nor do they provide data on the occurrence of multiple lesions per strand, a phenomenon recognized as highly detrimental to proper DNA function.[9]

In contrast, single-molecule sequencing methods such as nanopore ion channel detection[10] offer the potential to obtain both the identity and the sequence context of base damage sites on individual DNA strands as they translocate through the ion channel. Presently this method is focused on detection of the sequence of the native DNA bases (adenine (A), thymine (T), cytosine (C), and guanine (G)), in order to provide rapid genomic sequencing.[11−17] However, sequencing methods based on translocation of DNA through ion channels, as well as solid-state pores, have proved problematic due to insufficient current resolution between the native bases.[11,13−15,18] It has previously been shown that single-stranded DNA (ssDNA) molecules can be captured and immobilized within an α-hemolysin (α-HL) ion channel by linking a biotin (Btn) molecule directly to the DNA 3′ terminus and binding the DNA conjugate to streptavidin (Strep), as the streptavidin is too large to pass the α-HL channel.[19−23] As a result of this immobilization technique, the longer residence time of the DNA molecule within the α-HL channel circumvents many of the issues involved with ssDNA translocation, making it possible to distinguish not only the orientation of DNA entering the pore[19] but also a single change in the native base sequence.[22−25]

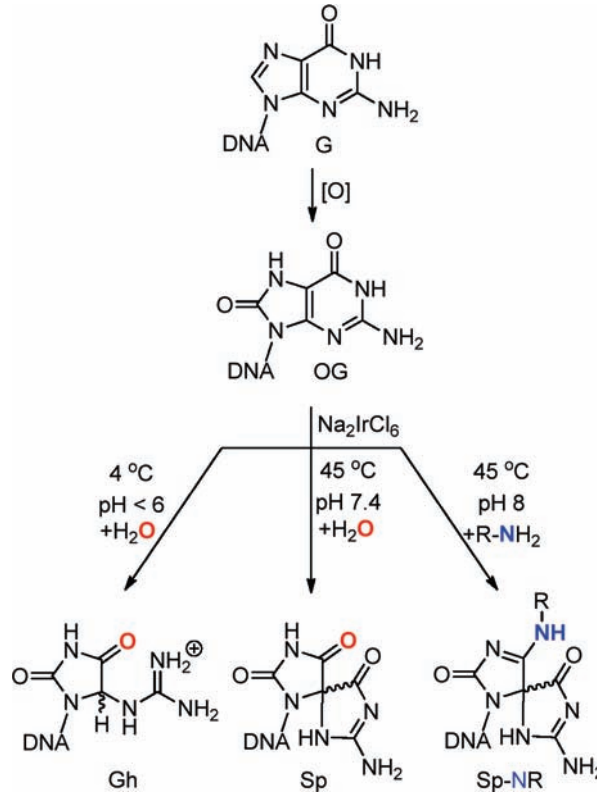

Figure 1. Oxidation of the biomarker OG leads to the hydantoins Sp and Gh, depending on pH and base stacking context. The oxygen shown in red is incorporated from H_2O; inclusion of primary amines during oxidation leads to covalent adducts at this site.

The method described above should also be applicable to single-molecule sequencing of DNA damage, for which no method currently exists, which has great importance in medicinal diagnostics and in understanding the origins of diseases. Herein, we describe the detection of a single oxidative base lesion within a background of surrounding native bases by immobilizing ssDNA in an α-HL ion channel.

10.1021/ja109501x

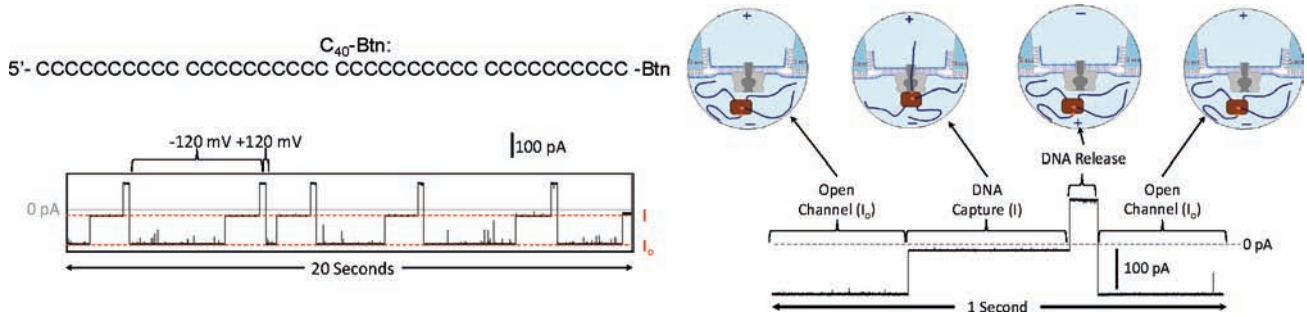

Figure 2. Strep-Btn-C_{40} structure, example $i-t$ trace, and molecule capture/release schematic. A C_{40} ssDNA strand is tethered to a Btn molecule on the 3′ end, and for strand immobilization within the αHL channel, the Btn-DNA is bound to Strep. Schematic not drawn to scale.

Because OG is similar in size and shape to the parent base G, we elected to magnify the difference between the two by taking advantage of the greatly reduced redox potential of OG compared to G (0.74 and 1.29 V vs NHE, respectively[26]), which results in a high reactivity of OG toward further oxidation. The mild, water-soluble oxidants ferricyanide and hexachloroiridate oxidize OG selectively in a strand of DNA leading to hydantoin lesions, particularly spiroiminodihydantoin (Sp)[27] when the oxidation of ssDNA is carried out at pH 8.[28] When a primary amine, such as lysine or spermine (Spm), is present during oxidation, an oxidized intermediate is trapped by the nucleophilic amine, generating a covalent adduct to OG as a spirocyclic adduct (Sp-NR) (Figure 1).[29,30]

Single oxidized base modifications, as outlined in Figure 1, were placed within a homopolymer poly-dC background sequence and in the K-*ras* heterosequence. Both sequences were examined for single base oxidative damage through ion channel recordings. The DNA immobilization technique introduced by the Bayley and Schmidt laboratories[22,23] was applied to the experiments presented here, carried out using a wild-type α-HL ion channel reconstituted within a lipid bilayer suspended across a glass nanopore membrane.[31−33]

In the present work, we demonstrate that a simple chemical derivatization of OG to form hydantoin adducts of various sizes can lead to a nearly 10% change in the ion channel blockage current, not only for homopolymer sequences but for heterosequences as well, providing an excellent entry into the single-molecule sequencing of this oxidized lesion. To our knowledge, this is the first presentation of the ability to detect and identify singe-point base lesions within homo- and heteropolymer native base sequences through ion channel recordings.

A single wild-type α-HL protein ion channel was reconstituted into a 1,2-diphytanoyl-*sn*-glycero-3-phosphocholine lipid bilayer suspended across the orifice of a glass nanopore membrane (GNM), with an orifice radius between 500 and 1000 nm. The GNM provides a robust bilayer support with low electrical noise.[31−33] Because the translocation of ssDNA through α-HL is too fast for accurate single-base identification, we immobilized ssDNA oligomers within the ion channel via a tethered biotin−streptavidin (Strep-Btn) complex (Figure 2).[22,23]

A voltage was applied across the α-HL ion channel to electrophoretically drive the Strep-Btn DNA complex into the α-HL ion channel, where it was held for 1−2 s to collect current blockage event data. It was then released by reversing the voltage bias, which drives the Strep-Btn DNA into the bulk solution, restoring the open-channel current. Figure 2 shows a typical current−time ($i-t$) trace for the capture of Strep-Btn-C_{40} (hereinafter termed "C_{40}"). When −120 mV was applied (*cis* vs *trans*), an open-channel current level, I_o, and current blockage level, I, were observed when the channel was unblocked and blocked by C_{40}, respectively. This capture and release cycle was repeated to collect a population of current blockage events (>100 events) for multiple and different DNA strands within the sample of interest. The schematic in Figure 2 illustrates the open-channel, capture, release, and open-channel cycle for the Strep-Btn immobilization experiment; brief current fluctuations in the open-channel current are attributed to noise and unbound ssDNA. All voltages were applied *cis* vs *trans* with respect to the α-HL channel (corresponding to external vs internal solutions with respect to the GNM).

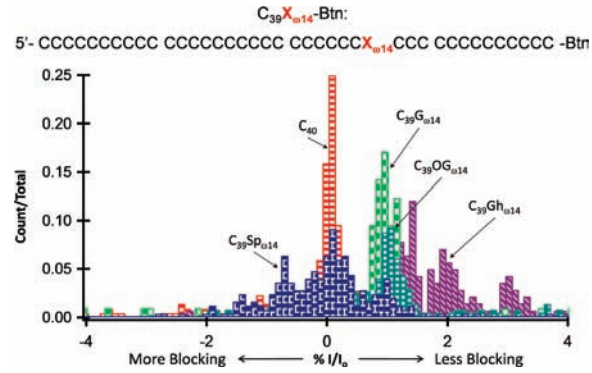

Figure 3. Current blockage histograms comparing guanine (G), 8-oxo-7,8-dihydroguanine (OG), spiroiminodihydantoin (Sp), and guanidinohydantoin (Gh) at position ω14 relative to C_{40}. All oxidation products are within a poly-dC background, $C_{39}X_{\omega 14}$. C_{40} is used as a reference sample; the $\%I/I_o$ for C_{40} was set equal to 0, and $\%I/I_o$ for all other samples is relative to C_{40}.

Previous work has shown that the native base at position 14, relative to the 3′ terminus (ω14) in the DNA strand, has a particularly sensitive influence on the K^+ and Cl^- ion flux in the β-barrel sensing region of α-HL.[22] The DNA lesions under study were initially incorporated into the ω14 position of a poly-dC background with a total length of 40 nucleotides. The ion channel current blockage level of the base lesions at this position was evaluated relative to the unmodified, homopolymer sequence C_{40}.

Our initial efforts focused on defining the electrical signature of a single oxidized guanine lesion suspended within the α-HL channel. Figure 3 shows histograms of the percent blockage current when G at position ω14, in a poly-dC background, was substituted by OG or by the further oxidation product Sp or Gh (guanidinohydantoin) (see the Supporting Information for individual $i-t$ traces and $\%I/I_o$ histograms relative to C_{40} and native bases). C_{40} was used as a reference, and current blockage for all molecules is reported referenced to the blockage level of C_{40}, which is assigned a value of $\%I/I_o = 0$; all experiments were reproduced at least once, and peak positions relative to C_{40} are consistent in position (within 0.1%). In the poly-dC sequence context, G is about 1.2% less blocking than C, and OG yields an electrical signature nearly

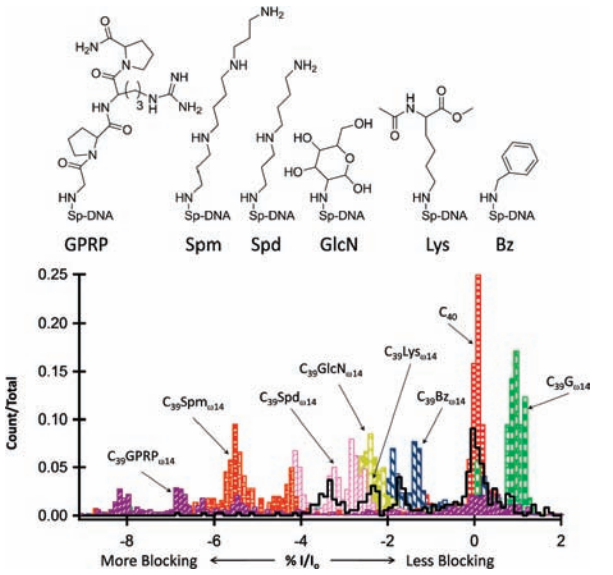

Figure 4. %I/I_o histograms comparing benzylamine (Bz), lysine (Lys), glucosamine (GlcN), spermidine (Spd), spermine (Spm), and Gly-Pro-Arg-Pro amide (GPRP) adducts at position ω14 relative to C_{40}. All adducts are within a poly-dC background, $C_{39}X_{\omega 14}$. C_{40} was used as a reference sample; the %I/I_o for C_{40} was set equal to 0, and %I/I_o for all other samples is relative to C_{40}.

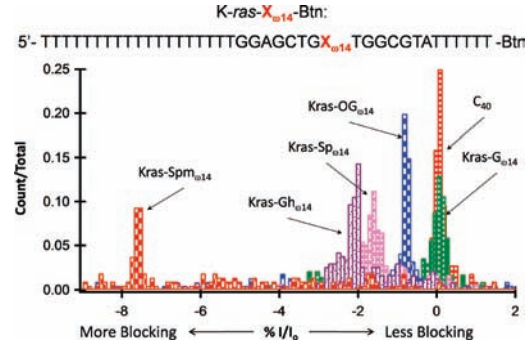

Figure 5. %I/I_o histograms for G, OG, Sp, Gh, and Spm base modifications at position ω14 relative to C_{40}. All adducts are within a poly-dT background, Btn-K-*ras*-$X_{\omega 14}$. C_{40} was used as a reference sample; the %I/I_o for C_{40} was set equal to 0, and %I/I_o for all other samples was relative to C_{40}. The %I/I_o peak positions relative to C_{40} and among modified DNA molecules have shifted blocking order compared with modifications within a homopolymer background, indicating that the current blockage level is not only influenced by the modification itself but also the surrounding sequence.

identical to that of G. The hydantoin products Sp and Gh are shifted from G and OG and display broader histograms, possibly due to the formation of diastereomeric pairs for each of these products as well as multiple conformations that might exist due to poor base stacking of hydantoins compared to normal bases.

Although the oxidative lesions OG, Sp, and Gh give current blockage signatures significantly different from that of the native G base, we hypothesized that even larger spirocyclic adducts (Sp-X) created by the oxidation of OG in the presence of a primary amine (Figure 1) would modulate the ion channel current to an even larger extent. The amines selected to form adducts were chosen to modify the size and geometry of the DNA strand at position ω14.

Amine adducts introduced at position ω14 within the poly-dC background, $C_{39}X_{\omega 14}$, included benzylamine (Bz), lysine (Lys), glucosamine (GlcN), spermidine (Spd), spermine (Spm), and Gly-Pro-Arg-Pro amide (GPRP). Figure 4 shows the structures for the spirocyclic adducts mentioned above and the %I/I_o histograms relative to C_{40} (see the Supporting Information for individual $i-t$ traces and %I/I_o histograms for spirocyclic adducts relative to C_{40} and native bases). The $C_{39}Spd_{\omega 14}$ and $C_{39}Spm_{\omega 14}$ adducts are long, linear, and flexible adducts, and both produce multiple, more blocking %I/I_o peaks compared with $C_{39}G_{\omega 14}$, blocking up to 5% and 7% more current, respectively. Spm, being the larger adduct compared with Spd, produced the deepest current blockades. $C_{39}Lys_{\omega 14}$ produced multiple current blockage levels, with %I/I_o peaks spread over a large range, roughly 1−5% more blocking than $C_{39}G_{\omega 14}$, with a prominent peak on top of C_{40}. The $C_{39}Lys_{\omega 14}$ peak, which is approximately 1% more blocking than that of $C_{39}G_{\omega 14}$, has an %I/I_o peak position and distribution similar to those of $C_{39}Sp_{\omega 14}$ (Figure 3), possibly a result of Lys having been hydrolyzed to Sp. The bulky spirocyclic adducts produced the most variable current blockage signals. For example, $C_{39}Bz_{\omega 14}$, $C_{39}GlcN_{\omega 14}$, and $C_{39}GPRP_{\omega 14}$ all resulted in deeper current blockades compared with $C_{39}G_{\omega 14}$, and all produced signals with a broad distribution of current blockage levels and noise amplitudes (see the Supporting Information). The various current blockage levels and noise amplitudes are thought to be associated with cyclic adducts adopting different conformations within the α-HL channel.

$C_{39}Bz_{\omega 14}$ and $C_{39}GlcN_{\omega 14}$ produced an approximately 3 and 4% negative shift in %I/I_o, respectively, relative to $C_{39}G_{\omega 14}$. The $C_{39}GPRP_{\omega 14}$ adduct produced events with the deepest current blockades, up to 10% compared with $C_{39}G_{\omega 14}$, but the distribution was very broad and contained a prominent population of events with current blockage levels similar to that of C_{40}. This is interpreted to suggest the molecule is not readily entering the sensing regions of the channel, resulting in a current blockage signal arising from the surrounding poly-dC sequence. To further test the ability to detect oxidative damage within a natural DNA sequence, base modifications were examined within an immobilized heterosequence.

The oxidatively damaged species OG, Sp, and Gh, as well as the spermine adduct to OG (Spm), were selected for immobilization studies within a heterosequence background to determine the extent to which a DNA damage site can be detected in a sequence of biological relevance. These lesions permit the study of primary DNA damage products as well as a simple adduct to OG (Spm), all of which produced strong %I/I_o peaks rather than a dispersed population of blockage currents. The heterosequence selected for study was a portion of the K-*ras* gene near codon 12 embedded in a poly-dT background while maintaining the 40-mer length (Figure 5). A poly-dT background is used to avoid secondary structures which occur as the poly-dC interacts with the G-rich K-*ras* sequence. Point mutations within codon 12 of the K-*ras* proto-oncogene have been shown to cause uncontrolled cell growth and loss of cell differentiation, leading to various human adenocarcinomas.[34]

Specifically, in lung cancer, the K-*ras* gene predominantly undergoes a G → T transversion mutation (GGT → GTT) that could result from the failure to repair guanine oxidative damage before replication.[34,35] Thus, we positioned the K-*ras* sequence within the α-HL channel in such a way that the central G of codon 12, or its oxidized derivatives, was located at the ω14 position. Results for detecting the native gene sequence (K-*ras*-$G_{\omega 14}$) and oxidation products OG (K-*ras*-$OG_{\omega 14}$), Sp (K-*ras*-$Sp_{\omega 14}$), and Gh (K-*ras*-$Gh_{\omega 14}$), as well as the Spm adduct (K-*ras*-$Spm_{\omega 14}$), are displayed in Figure 5.

When comparing the %I/I_o peaks for modifications within the poly-dC background against the K-*ras* sequence, it is apparent that the surrounding sequence has a profound influence on the current signature and event population distribution. Specifically, K-*ras*-

$G_{\omega 14}$ and *K-ras*-$OG_{\omega 14}$ produced $\%I/I_o$ peaks separated by approximately 1% from each other, with the K-*ras*-$G_{\omega 14}$ producing the lesser blockage. Whereas G and OG produced overlapping histograms in the C_{40} background, their signatures are quite distinct and show narrower distributions in the K-*ras* sequence. K-*ras*-$Sp_{\omega 14}$ resulted in a single, strong $\%I/I_o$ peak, approximately 1.5% more blocking than K-*ras*-$G_{\omega 14}$ and again distinct from the OG signal; in the poly-dC background, the Sp oxidation product produced a dispersed population of current blockage levels yielding multiple $\%I/I_o$ peaks with positions similar to those of C_{40}, $C_{39}G_{\omega 14}$, and $C_{39}OG_{\omega 14}$. The K-*ras*-$Gh_{\omega 14}$ sample produced the greatest change from its $C_{39}Gh_{\omega 14}$ analogue: K-*ras*-$Gh_{\omega 14}$ has a single $\%I/I_o$ peak approximately 2% more blocking compared with that of K-*ras*-$G_{\omega 14}$. In the poly-dC background, the Gh oxidation product produced multiple $\%I/I_o$ peaks that are 0.5−2% less blocking than those of $C_{39}G_{\omega 14}$.

Although $\%I/I_o$ peak position, dispersion, and relative amplitude are sequence dependent, if the structural modification is large enough, the current blockade from the modification will dominate the influence from the surrounding sequence. The spermine adduct now proves to be such a modification, as it consistently produced a more blocking $\%I/I_o$ peak shift of around 8% relative the unmodified ($G_{\omega 14}$) sequence in both the K-*ras* and poly-dC backgrounds. Overall, $\%I/I_o$ peaks appear sharper and less dispersed for oxidation products and adducts within the K-*ras* sequence than when present in the poly-dC background.

The immobilization studies presented above are preliminary experiments toward translocation studies; it will be necessary to examine the most blocking adducts for the ability to readily pass through the constriction of α-HL and translocate the pore. It was previously demonstrated by the Howorka laboratory that peptide tags can be used to change the current blockage amplitude and event duration of translocating DNA strands,[36,37] and by the same principle, manipulating the size, geometry, and electrical characteristics of the DNA damage site should lead to detection via nanopore translocation. Future works will focus on characterizing those adducts that most readily distinguish ssDNA strands with oxidative damage from undamaged strands. The translocation for adducts will be evaluated for unique current blockage levels, current signatures, event durations, and translocation velocities as a function of applied voltage and reported at a later date.

These initial studies have shown the power of ion channel recordings for the detection of DNA damage and highlighted the ability to detect a single lesion within both homo- and heteropolymer DNA sequences. We have taken a first step toward damage detection through ion channel recording translocation experiments. In addition to being able to detect DNA damage, this work has introduced many options for identifying the damage, as each adduct produced a unique current blockage level and/or population distribution and noise signature, with a general trend of larger adducts producing the most blocking current blockage levels.

Acknowledgment. This work was supported by a seed grant from the University of Utah as well as funds from the NIH (HG005095). Instruments and software donated by Electronic Bio Sciences, San Diego, are gratefully acknowledged as well as helpful discussions with Drs. Geoffrey Barrall, Eric Ervin, and John Watkins of EBS. The authors thank Dr. James Muller (University of Utah) for assistance with mass spectrometry.

Supporting Information Available: Experimental methods for synthesis, purification, and characterization of all oligomer adducts; immobilization $i-t$ traces and $\%I/I_o$ histograms; native base immobilization $\%I/I_o$ histograms; and complete ref 10. This material is available free of charge via the Internet at http://pubs.acs.org.

References

(1) Cooke, M. S.; Olinski, R.; Evans, M. D. *Clin. Chim. Acta* **2006**, *365*, 30–49.
(2) Cadet, J.; Douki, T.; Ravanat, J.-L. *Free Radic. Biol. Med.* **2010**, *49*, 9–21.
(3) Delaney, J. C.; Essigmann, J. M. *Chem. Res. Toxicol.* **2008**, *21*, 232–252.
(4) Gedik, C. M.; Collins, A. *FASEB J.* **2005**, *19*, 82–84.
(5) Mangal, D.; Vudathala, D.; Park, J.-H.; Lee, S. H.; Penning, T. M.; Blair, I. A. *Chem. Res. Toxicol.* **2009**, *22*, 788–797.
(6) Azqueta, A.; Shaposhnikov, S.; Collins, A. R. *Mutat. Res.* **2009**, *674*, 101–108.
(7) Cadet, J.; Poulsen, H. *Free Radic. Biol. Med.* **2010**, *48*, 1457–1459.
(8) Muller, J. G.; Duarte, V.; Hickerson, R. P.; Burrows, C. J. *Nucleic Acids Res.* **1998**, *26*, 2247–2249.
(9) Hada, M.; Sutherland, B. M. *Radiat. Res.* **2006**, *165*, 223–230.
(10) Branton, D.; et al. *Nat. Biotechnol.* **2008**, *26*, 1146–1153.
(11) Kasianowicz, J. J.; Brandin, E.; Branton, D.; Deamer, D. W. *Proc. Natl. Acad. Sci. U.S.A.* **1996**, *93*, 13770–13773.
(12) Akeson, M.; Branton, D.; Kasianowicz, J. J.; Brandin, E.; Deamer, D. *Biophys. J.* **1999**, *77*, 3227–3233.
(13) Meller, A.; Nivon, L.; Brandin, E.; Golovchenko, J.; Branton, D. *Proc. Natl. Acad. Sci. U.S.A.* **2000**, *97*, 1079–1084.
(14) Deamer, D. W.; Branton, D. *Acc. Chem. Res.* **2002**, *35*, 817–825.
(15) Fologea, D.; Gershow, M.; Ledden, B.; McNabb, S. D.; Golovchenko, J. A.; Li, J. *Nano Lett.* **2005**, *5*, 1905–1909.
(16) Astier, Y.; Braha, O.; Bayley, H. *J. Am. Chem. Soc.* **2006**, *128*, 1705–1710.
(17) Clarke, J.; Wu, H.-C.; Jayasinghe, L.; Patel, A.; Reid, S.; Bayley, H. *Nat. Nanotechnol.* **2009**, *4*, 265–270.
(18) Meller, A.; Nivon, L.; Branton, D. *Phys. Rev. Lett.* **2001**, *86*, 3435–3438.
(19) Henrickson, S. E.; Misakian, M.; Robertson, B.; Kasianowicz, J. J. *Phys. Rev. Lett.* **2000**, *85*, 3057–3060.
(20) Nakane, J.; Wiggin, M.; Marziali, A. *Biophys. J.* **2004**, *87*, 615–621.
(21) Purnell, R. F.; Mehta, K. K.; Schmidt, J. J. *Nano Lett.* **2008**, *8*, 3029–3034.
(22) Stoddart, D.; Heron, A. J.; Mikhailova, E.; Maglia, G.; Bayley, H. *Proc. Natl. Acad. Sci. U.S.A.* **2009**, *106*, 7702–7707.
(23) Purnell, R. F.; Schmidt, J. J. *ACS Nano* **2009**, *9*, 2533–2538.
(24) Stoddart, D.; Maglia, G.; Mikhailova, E.; Heron, A. J.; Bayley, H. *Angew. Chem., Int. Ed.* **2009**, *48*, 1–5.
(25) Wallace, E. V. B.; Stoddart, D.; Heron, A. J.; Mikhailova, E.; Maglia, G.; Donohoe, T. J.; Bayley, H. *Chem. Commun.* **2010**, *46*, 8195–8197.
(26) Steenken, S.; Jovanovic, S. V.; Bietti, M.; Bernhard, K. *J. Am. Chem. Soc.* **2000**, *122*, 2372–2374.
(27) Luo, W.; Muller, J. G.; Rachlin, E. M.; Burrows, C. J. *Org. Lett.* **2000**, *2*, 613–617.
(28) Kornyushyna, O.; Berges, A. M.; Muller, J. G.; Burrows, C. J. *Biochemistry* **2002**, *41*, 15304–15314.
(29) Hosford, M. E.; Muller, J. G.; Burrows, C. J. *J. Am. Chem. Soc.* **2004**, *126*, 9540–9541.
(30) Xu, X.; Muller, J. G.; Ye, Y.; Burrows, C. J. *J. Am. Chem. Soc.* **2008**, *130*, 703–709.
(31) Zhang, G.; Zhang, Y.; White, H. S. *Anal. Chem.* **2004**, *76*, 6229–6238.
(32) Zhang, B.; Galusha, J.; Shiozawa, P. G.; Wang, G.; Bergren, A. J.; Jones, R. M.; White, R. J.; Ervin, E. N.; Cauley, C. C.; White, H. S. *Anal. Chem.* **2007**, *79*, 4778–4787.
(33) White, R. J.; Ervin, E. N.; Yang, T.; Chen, X.; Daniel, S.; Cremer, P. S.; White, H. S. *J. Am. Chem. Soc.* **2007**, *129*, 11766–00775.
(34) Pfeifer, G. P.; Besaratinia, *Hum. Genet.* **2009**, *125*, 493–506.
(35) David, S. S.; O'Shea, V. L.; Kundu, S. *Nature* **2007**, *447*, 941–950.
(36) Mitchell, N.; Howorka, S. *Angew. Chem., Int. Ed.* **2008**, *47*, 5565–5568.
(37) Borsenberger, V.; Mitchell, N.; Howorka, S. *J. Am. Chem. Soc.* **2009**, *131*, 7530–7531.

JA109501X